



Controlled release starch-lipid implant for the therapy of severe malaria

Golbarg Esfahani^a, Olaf Häusler^b, Karsten Mäder^{a,*}

^a Institute of Pharmacy, Martin Luther University Halle-Wittenberg, Kurt-Mothes-Straße 3, 06120 Halle (Saale), Germany

^b Roquette Freres, route haute loge, 62080 Lestrem, France

ARTICLE INFO

Keywords:

Controlled release
Biodegradable
Starch
Glycerol monostearate
Artesunate
Artemether

ABSTRACT

Parenteral depot systems can provide a constant release of drugs over a few days to months. Poly-(lactic acid) (PLA) and Poly-(lactide-co-glycolide) (PLGA) are the most commonly used polymers in the production of these systems. Finding alternatives to these polymers is of great importance to avoid certain drawbacks of these polymers (e.g. microacidity) and to increase the selection possibilities. In this study, different types of starch in combination with glycerol monostearate (GMS) were developed and investigated for their physicochemical properties and release characteristics. The noninvasive method of electron paramagnetic resonance (EPR) was used to study the release kinetics and mechanisms of nitroxide model drugs. The studies demonstrated the general suitability of the system composed of high amylose starch and GMS to form a controlled release system. For further characterization of the prepared system, formulations with different proportions of starch and GMS, loaded with the antimalarial agents artesunate or artemether were prepared. The implants were characterized with X-ray powder diffraction (XRPD) and texture analysis. The *in vitro* release studies demonstrated the sustained release of artemether over 6 days from a starch-based implant which matches desired kinetic for the treatment of severe malaria. In summary, a starch-based implant with appropriate mechanical properties was produced that can be a potential candidate for the treatment of severe malaria.

1. Introduction

Parenteral depot systems are potential drug delivery systems for the treatment of various diseases. They have several advantages compared to oral administration, because these systems can provide a constant concentration of the drug for a few days to several months. Many of the drugs with low water solubility and short half-life are good candidates to be loaded in these systems (Kempe and Mäder, 2012). In the last two decades, there has been a growing interest in long acting parenteral drug delivery systems. Currently, various types of parenteral depot systems are commercially available on the pharmaceutical market. Most of these products are based on polylactic acid (PLA) and poly(lactic-co-glycolic) acid (PLGA) polymers. PLA and PLGA are biodegradable polymers. However, they degrade to acidic monomers which might cause acidic microenvironments both *in vitro* (Ding and Schwendeman, 2008) and *in vivo* (Mäder et al., 1996; Schädlich et al., 2014). In addition to the development of low PH values inside the degrading polymer matrix, these acidic monomers can also cause autocatalysis and complex and nonlinear release profiles. Also, drug inactivation may happen by the formation of the covalent bond between the drug molecule and the

produced monomers (Lucke et al., 2002). Hence, finding alternative biodegradable materials will be beneficial in the formulation of future parenteral depot systems. Starch, as a natural biodegradable polymer can be a candidate to replace these polymers.

Starch (nonmodified form) is in general fully biodegradable. Its degradation in the body produces non-toxic and non-acidic monomers (Araújo et al., 2004). Starch-based materials are already clinically used as bioresorbable medical products for providing hemostasis and to prevent postoperative tissue adhesion (Krämer et al., 2021; Mendes et al., 2001). It is also a major excipient in the pharmaceutical industry. However, there are still some drawbacks in using starch; such as its weak mechanical properties and its fast degradation in the body over a few days. Starch properties can be modified by the presence of other molecules and/or the impact of temperature and pressure. Studies have shown that starch can form complexes with certain lipids (e.g. fatty acids or mono-glycerides) and lipid complexation can be facilitated at higher temperatures utilizing the extrusion process (De Pilli et al., 2016). In this study, the effect of the addition of the lipid to starch and the effect of temperature and pressure on starch was evaluated to modify starch characteristics. In addition, the formation of starch-lipid complexes

* Corresponding author.

E-mail address: karsten.maeder@pharmazie.uni-halle.de (K. Mäder).

<https://doi.org/10.1016/j.ijpharm.2022.121879>

Received 16 February 2022; Received in revised form 9 May 2022; Accepted 26 May 2022

Available online 29 May 2022

0378-5173/© 2022 The Authors. Published by Elsevier B.V. This is an open access article under the CC BY license (<http://creativecommons.org/licenses/by/4.0/>).

makes the material more resistant against enzymatic digestion (Cui and Oates, 1999; Gelders et al., 2005). Introducing lipids into starch is therefore a rational approach to decrease enzymatic degradation and to slow down the drug release.

Malaria is a life-threatening disease. Despite recent efforts to reduce the malaria burden globally, there were an estimated 229 million clinical cases, 2 million severe malaria cases, and approximately 409 000 deaths due to malaria worldwide in 2019 (World Health Organization, 2020). Artesunate (AS) is the WHO first-line treatment of severe malaria in adults and children. It is a clinically versatile artemisinin derivative but with an extremely short half-life. Per WHO guidelines, this drug should be administered several times per day intravenously in case of treatment of severe malaria. Studies have shown that intravenous artesunate administration is associated with high initial artesunate concentrations which subsequently decline rapidly, with typical artesunate half-life estimates of less than 15 min (Morris et al., 2011). Per WHO guidelines, parenteral artemether (AM) is an alternative option in case injectable artesunate is not available (World Health Organization, 2015). Both of these drugs are metabolized to dihydroartemisinin (DHA), the active metabolite of the drugs, in the human body. Artemether is poorly soluble in water and its parenteral formulation is only available as a premixed oil-based solution for intramuscular injection (Esu et al., 2020). Based on a WHO report, intramuscular injection of artemether results in slow but erratically absorption that leads to a smaller survival benefit than intravenously applied artesunate (World Health Organization, 2015). Therefore, finding a system that provides a sustained release of artesunate or artemether is of great clinical importance to treat severe malaria. The aim of this study was the preparation and characterization of a parenteral depot system based on starch and lipid that can provide a constant release of artesunate or artemether over a few days to a week for the treatment of severe Malaria.

This study is divided into two main parts. In prescreening studies, implants with different types of starch in combination with Glycerol monostearate (GMS) were produced and characterized to find the appropriate type of starch and lipid to be used. The homogeneity of the prepared implants and their physical stability in PBS were the criteria for the selection of the implants for further assessment by Electron Paramagnetic Resonance (EPR). The implant's microenvironment, water penetration into the implants, and release behavior of model drugs from the implants were assessed with EPR. Based on the obtained data from prescreening studies, three formulations were chosen to load antimalarial agents. The prepared implants were characterized by texture analysis, X-ray powder diffraction, and high-pressure liquid chromatography (HPLC).

2. Materials and methods

2.1. Materials

Native pea starch (PEA STARCH N-735) and high amylose starch (MAIZE STARCH AMYLO N-400 (amylose content \approx 53%)) were kindly provided by Roquette (Lestrem, France). Hydroxyethyl starch (HES) was kindly provided by Serumwerk Bernburg (Bernburg, Deutschland). Glycerol monostearate (Kolliwax® GMS II) was kindly provided by BASF (Germany). Glycerol monostearate (IMWITOR® 491) was kindly provided by IOI Oleo GmbH (Germany). Tempol (4-Hydroxy-TEMPO) and Tempol Benzoate (4-hydroxy-tempo benzoate) were purchased from SIGMA Aldrich Chemie GmbH (Munich, Germany). Artemether and artesunate were purchased from abcr GmbH. Olive oil was purchased from Caelo (Germany). NMP (1-Methyl-2-pyrrolidone) was purchased from Sigma-Aldrich (USA). Testing media was Phosphate Buffered Saline (Ph.Eur.) plus 1% sodium dodecyl sulfate (SDS), adjusted to pH 7.4. SDS was purchased from Sigma Aldrich Chemie GmbH (Munich, Germany). Acetonitrile (VWR International, Darmstadt, Germany), Formic Acid (Merck, Germany) and, double distilled water were used for the HPLC measurements.

2.2. Prescreening studies

Prescreening studies were conducted to identify the appropriate type of starch that can form a controlled release system in combination with lipid (GMS). Also, the temperature and extrusion speed for the HME process and the amount of water in the formulation were optimized in prescreening studies. Four different types of starch including HES, native pea starch, gelatinized pea starch, and high amylose starch in combination with two commercially available products of Glycerol monostearate (GMS) namely Kolliwax® GMS II and IMWITOR® 491 were examined. Gelatinized pea starch was obtained by adding water to pea starch (1 g pea starch:5 g water) and stirring the mixture at 80 °C for 5 min. The preparation was then dried in an oven at 50 °C overnight. The produced film was cryomilled with two 4 mm grinding media with two cycles each at 25 Hz for 90 s. The implants were prepared by hot-melt extrusion (ZE 5 ECO; Three-Tec GmbH; Seon; Swiss) with different extrusion screw speeds and different temperatures zones, depending on the formulation's components. Thermal measurements were also conducted to assess the thermal behavior of the formulation; the data is shown in the supplementary materials (Fig. S1 and Fig. S2). The homogeneity of the implants was studied with optical light microscopy on the micrometer scale. The physical stability of the prepared implants was assessed by incubating extrudates of 1 cm length in 50 ml PBS, pH 7.4 at 37 °C in the shaker (Mettmert GmbH + Co. KG, Schwabach, Germany). The homogeneity of the prepared implants and their physical stability in PBS were the criteria for choosing the implants for further assessment by EPR.

2.3. Optical light microscopy

Light microscopy was used to assess the homogeneity of the prepared implant on the micrometer scale.

2.4. Hot melt extrusion

The following criteria led to the selection of the excipients and the processing conditions of extrusion. In general, extrusion the temperature should not be too high to prevent chemical degradation. However, if the temperature is too low, no extrusion is possible. Prescreening studies showed that a minimum temperature of around 60 °C is needed to obtain homogenous extrudates from starch. As the higher temperature than the melting point of the lipid may lead to the separation of the solid starch and the low viscous oily liquid, IMWITOR 491 with a higher melting point than Kolliwax® GMS II was chosen as the lipid component. Water which was used as a plasticizer plays a significant role in the extrusion process. Although a certain amount of water is needed to gelatinize the starch (what makes the extrudates more flexible) and make the extrusion possible, an excess amount of water leads to super soft extrudates which are hard to gather or even the formation of foam-like material. Also, it should be noted that the formulations containing a high amount of lipid were only extrudable with a lower amount of water. The water amount was optimized in prescreening studies. Based on the results of the prescreening studies high amylose starch (AMYLO N-400®) and GMS (IMWITOR® 491) were chosen to prepare the implants by hot-melt extrusion (HME) (ZE 5 ECO; Three-Tec GmbH; Seon; Swiss). The components of each formulation and the hot-melt extrusion parameters (including extrusion screw speed and heating zone temperatures) are shown in Table 1 and Table 2 respectively. Before extrusion, components of each formulation were mixed and filled into the grinding chamber of a Retsch CryoMill (Retsch, Haan, Germany) together with two 10 mm grinding media. The cryomilling process scheduled an automatic pre-cooling phase and 2 milling cycles at 30 Hz for 150 s. Each cycle was followed by a 30 s lasting cooling phase at 5 Hz. Extrusion dies with a 1 mm diameter were used. Samples were collected and stored in opaque falcon tubes between 4° and 8 °C.

Table 1

Composition of investigated formulations in gram.

Formulation No	Formulation name	Components [g]				
		High amylose maize Starch	GMS	Artemether	Artesunate	water
1	Starch implant	4	–	–	–	2
2	Starch-lipid implant	4	3	–	–	1
3	Starch-AM implant	5	–	5	–	2.5
4	Starch-AM-Low lipid implant	4	1	5	–	2
5	Starch-AM-High lipid implant	4	3	7	–	1
6	Starch-AS implant	5	–	–	5	2.5
7	Starch-AS-Low lipid implant	4	1	–	5	2
8	Starch-AS-High lipid implant	4	3	–	7	1

Table 2

Used extrusion parameters.

Formulation No.	Temp. heating zone 1 [°C]	Temp. heating zone 2 [°C]	Temp. heating zone 3 [°C]	Screw speed rpm
1	70	80	90	140
2	69	68	67	140
3	60	65	70	140
4	60	65	68	140
5	69	68	67	140
6	60	65	70	140
7	60	65	70	140
8	69	68	67	140

2.5. Electron paramagnetic resonance (EPR)

Electron paramagnetic resonance (EPR) was applied to assess the model drug release behavior, water penetration and the microenvironment in the blank formulations (No 1 and 2). Tempol and Tempol Benzoate (TB) were used as models for hydrophilic and hydrophobic drugs with a concentration of 5 mmol/kg. The implants were incubated in 50 ml PBS in a shaking water bath (50 rpm) at 37 °C. At determined time points, the implants were taken out of the PBS and transferred to the EPR spectrometer. EPR spectra were obtained using an L-Band spectrometer (Magnettech GmbH, Germany), operating at a microwave frequency of about 1.1–1.3 GHz, equipped with a re-entrant resonator. EPR parameters were set to: centre field 49 mT, scan width 12 mT, scan time 60 s, modulation amplitude 0.0625 mT and modulation frequency 100 kHz. The spectral simulation was used to determine the distribution of the spin probe between different phases. The software EPRSIM V.4.99 from the Biophysical laboratory EPR centre (Josef Stefan Institute of Solid State Physics Ljubljana, Slovenia) was used for the evaluation and simulation of the EPR spectra.

2.6. Texture analysis

The mechanical properties of the implants were studied by a texture analyzer (CT3-4500, Brookfield-Rheotec, Germany) with the TexturePro CT V1.6 software. The samples were placed on microscopic slides and adjusted at the base table (TA-RT-KIT) of the analyzer. The TA7 standard probe, which resembles a knife-edge, was utilized. The required force to push the probe with a constant velocity into the samples was measured. Experiments were conducted at 20 °C with a scan velocity of 0.05 mm/s and a trigger force of 0.067 N.

2.7. X-ray powder diffraction

XRPD was applied to determine the state of drugs and GMS inside the implants. As a preparation step for the XRPD measurements, the implants were split into smaller pieces with a scalpel and submitted to cryomilling (Retsch GmbH, Haan, Germany). After an automatic pre-cooling phase, samples were milled with two 4 mm grinding media at 25 Hz for 60 s. XRPD was performed on an STOE STADI MP (STOE & Cie

GmbH, Darmstadt, Germany) powder diffractometer, equipped with molybdenum anode (50 kV and 30 mA) and a Ge (1 1 1) monochromator to select the Mo K α radiation at 0.071073 nm. Data of the rotating samples were collected in the transmission mode from 2°–25° in 1° steps for 60 s each using a DECTRIS MYTHEN 1 K Strip Detector. The diffraction patterns obtained were processed using an STOE WinXPOW software package.

2.8. In vitro artemether and artesunate release

One centimeter implant of each formulation was weighed and placed in 2 ml vials filled with 1.5 ml PBS plus 1% SDS, pH 7.4 and the vials were slightly agitated in a shaker with light protection (Memmert GmbH + Co. KG, Schwabach, Germany) at 37 °C. Total buffer volume was withdrawn at regular time intervals and analyzed according to the described HPLC method. An appropriate volume of fresh PBS plus 1% SDS was replaced after taking samples. Each experiment was conducted in triplicate.

2.9. High performance liquid chromatography

HPLC analysis was performed with a Waters Delta 600 system with 717 plus Auto Sampler, 2996 Photodiode Array Detector, and a ZORBAX Eclipse XDB C8 150x4.6 5 μ m column. A sample volume of 40 μ l was injected at a flow rate of 1.0 ml/min. The mobile phase was Acetonitrile, water and formic acid with the ratio of 55:45:0.1 and 60:40:0.1 V/V for artesunate and artemether respectively. The retention times were 4.4 and 7.9 min for artesunate and artemether respectively. The quantification was carried out with a UV/VIS detector at 257 nm. Linear calibration curves ($r^2 > 0.999$) were obtained in the range of 50–1000 μ g/ml for both drugs. Masslynx V4.1 software was used to analyze the data.

3. Results and discussions

3.1. Prescreening studies

Starch is a widely used pharmaceutical excipient in its native and its modified forms (Sasaki et al., 2000). It can be used e.g. as a binder, disintegrant, diluent, glidant and lubricant (Builders et al., 2013). Native starches are coming from the different botanic origin and own therefore various physical properties, such as different gelatinisation temperatures. Choosing an appropriate starch type for a controlled release system is, therefore, an important goal of prescreening studies. It is also to consider that the pressure and the temperature of the HME process and the water amount, acting as a plasticizer in the formulation can alter the thermal properties of starch significantly (Bialleck and Rein, 2011; Castro et al., 2020; Donmez et al., 2021). This affects the implant mechanical properties. Therefore, finding an optimized temperature and extrusion speed, as well as the right water amount to prepare implants with appropriate mechanical properties, was another important goal of prescreening study.

The homogeneity of the prepared implants and their physical stability in PBS were the main criteria for choosing the right type of starch

and GMS. Results of prescreening studies did show, that more homogeneous extrudates were obtained with higher temperatures. GMS (Kollifix® GMS II) and GMS (IMWITOR® 491) have melting points of 58 °C and 68 °C respectively. When Kollifix® GMS II was used, high temperatures lead to the separation of GMS from the other components and its faster exit from the extruder. This was even worse in formulations with a higher amount of GMS. Therefore, GMS (IMWITOR 491) with a higher melting temperature was used as a lipid part of the formulation. Implants made of high amylose starch (AMYLO N-400®) and GMS (IMWITOR 491) were homogeneous and were physically stable in PBS for more than a month. Therefore, high amylose starch (AMYLO N-400®) and GMS (IMWITOR 491) were chosen to prepare the formulations for further studies.

3.2. Hot melt extrusion

Extrusion temperatures depend on the components of each formulation. The melting point of the GMS, homogeneity of the prepared implant, and drug stability were the determining factors in choosing the appropriate temperature for the process. If the temperature is too low, no extrusion is possible at all or inhomogeneous extrudates are formed. High temperatures can cause the formation of separated liquids (for GMS containing extrudates) and drug degradation (both artemether and artesunate are heat sensitive). Pure artemether has a melting point in the range of 86–89 °C (Kuntworbe et al., 2018). In order to prevent drug degradation, the maximum temperature of 70 °C was used for the formulations containing artemether or artesunate. As mentioned in prescreening studies, GMS (IMWITOR 491) with a higher melting point (68 °C) was used to make the extrusion process possible in higher temperatures for GMS containing samples. The finally applied process parameters for HME related to each formulation are listed in the Materials and Methods section in Table 2.

The starch implants loaded with artesunate (left) and artemether (right) are shown in Fig. 1.

3.3. Electron paramagnetic resonance

Electron paramagnetic resonance (EPR) was applied to evaluate the model drug release and the water penetration into the implants. A low frequency spectrometer (1.1 GHz, L-band) was used. L-band has the advantage of the higher penetrating depth of the irradiation (about 5–10 mm) into water-containing samples in comparison to X-band (Kempe et al., 2010). Stable nitroxyl radicals (spin probes) with different physicochemical properties allow the determination of micro-viscosity and micropolarity (Lurie and Mäder, 2005). In this study, Tempol (TL) and Tempol Benzoate (TB) as models of a hydrophilic (TL) and hydrophobic (TB) drug were used. The chemical structures of the spin probes are shown in Fig. 2.

The interaction with the nitrogen nucleus is the primary interaction of the unpaired electron in nitroxide spin probes. This interaction is called “hyperfine interaction”. Hyperfine interaction produces small changes in the allowed energy levels of the electron that leads to splitting the EPR signal into multiple lines. Tempol and Tempol benzoate

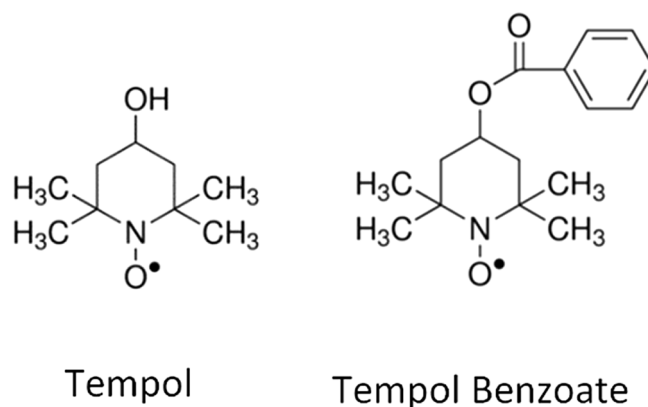


Fig. 2. Chemical structure of Tempol, (4-hydroxy-2,2,6,6-tetramethylpiperidine-N-oxyl, left) and Tempol benzoate (4-Hydroxy-2,2,6,8-tetramethylpiperidin-1-oxyl-benzoate, right).

with the predominant ^{14}N isotope give rise to a three-line EPR spectrum (Klug and Feix, 2008).

EPR spectra are sensitive to the rotational motion of the spin probes. Polarity and microviscosity are the parameters that affect the spin probe’s rotational motion and therefore the shape of the EPR spectra. Higher polarities cause larger distances between the lines of the spectra. As can be seen in Fig. 3, the distance between the outer lines in PBS as a

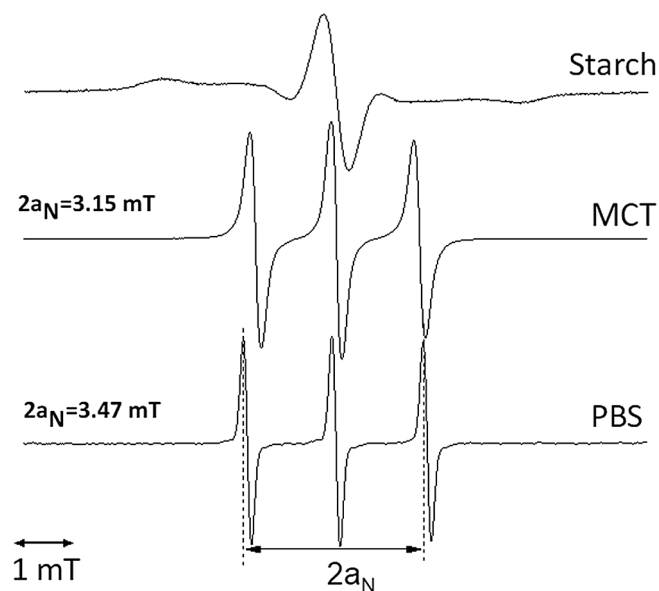


Fig. 3. EPR spectrum of TB in starch (powder-like spectrum), MCT (less polar environment, shorter distance between the outer lines, $2a_N = 3.15$ mT) and PBS (polar environment with longer distance between the outer lines, $2a_N = 3.47$ mT).

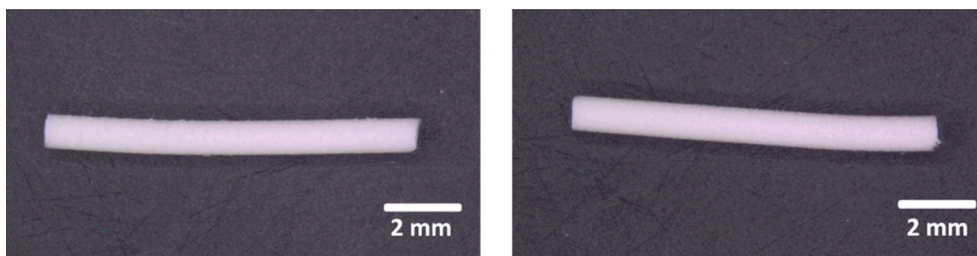


Fig. 1. Starch implants loaded with artesunate (left) and artemether (right) with 1 mm diameter.

polar environment is higher than the distance in medium chain triglyceride (MCT) as a less polar media (Lurie and Mäder, 2005). In low viscous media, the spin probes tumble freely resulting in spectra with three narrow lines of approximately equal height that can be seen in spectra of TB in PBS. As the viscosity increases, due to slower motions, the lines broaden and the signal amplitude decreases (Besheer et al., 2006). In a solution, anisotropic interactions are averaged out and lines widths are more narrow compared to less mobile and more viscous systems. In solid materials, the anisotropy is not averaged and typical “powder spectra” can be recorded (Evans et al., 2005; Kempe et al., 2010). EPR spectrum of TB loaded implant made of starch shows a “powder spectra” due to immobilization of TB inside the solid system.

Fig. 4 shows the EPR spectra of TB loaded implants in the dry state and after different times of exposure to PBS. The EPR spectra of TB in different components of the formulations were also obtained to achieve more details (Fig. S3). The EPR spectra are magnified by the mentioned number next to each signal to make the comparison easier. A decrease in signal amplitude of both implants was observed over two weeks shows the extended release of the TB from both implants. Comparing the two implants, it can be seen that the starch implant signal amplitude is almost one third after 9 days, while the signal amplitude of starch-lipid implant is about half after 15 days of PBS exposure. Therefore, as it was expected, a longer release time was observed in a formulation containing lipid (GMS). This is probably due to slower water penetration into the starch-lipid system in comparison to the starch system. The release of TB from the starch implant was almost completed after 14 days. After this time, only a very noisy signal was observed, due to the very low remaining amount of TB inside the implant. In contrast, no more decrease in the signal amplitude of starch-lipid implant was observed after the 15th day. This is probably due to some part of the TB that is trapped in the lipid part of the implant and it is not released from the system during this time period *in vitro*. Therefore, the addition of the lipid to the formulation could help to have the release of TB over a longer period of time.

To have a better understanding of the water penetration into the implant and also to determine the distribution of the spin probe between different phases, spectral simulations were carried out. The EPR spectra of TB in different environments and the simulations (dashed line) of the spectral pattern are shown in the supplementary in Fig. S4. Fig. 5 shows EPR spectra of TB loaded starch-lipid implant exposed to PBS (black line) after different exposure times to PBS and simulations (dashed line) of the mobile and immobile spectral pattern. A superposition of two species within the spectra was detectable. At all times, some part of TB is immobilised within the implant and its mobility is so restricted that so-called powder-like spectra result. In addition, a second species with higher mobility is observed which shows a three line spectrum with broad lines. The spectral shape indicates a “moderate” mobility which

means that the molecule is sufficient mobile to give some averaging of the anisotropic hyperfine splitting. However, the different amplitudes and broad line widths indicate much less mobility compared to low viscous systems (e.g. TB in water). After 5 min about 28% of the total amount of TB in the implant is moderate mobile and 72% of TB is still immobile. Over time, the amount of partially mobile TB inside the implant is increased due to the diffusion of water into the implant. Since the mobile TB is released from the implant into the PBS over time, a decrease in the amount of mobile TB was observed after 48 h. It should be noted that the mobile species of TB is still much less mobile compared to mobile Tempol in the corresponding starch and starch/lipid extrudates (Fig. 6). This can be concluded by comparison in the line width of the two spectra (Fig. 7). The three lines are much broader in TB mobile species spectra in comparison to the lines of the Tempol loaded implant spectra. As mentioned previously, slower motions of the spin probe broaden the lines of the EPR spectra.

In the next step, Tempol, as a hydrophilic spin probe was used to assess the water penetration into the implants in more detail. The EPR spectra of TL in olive oil (less polar environment, shorter distance between the outer lines), NMP and PBS (polar environment with longer distance between the outer lines) are shown in Fig. S5 (supplementary materials) as controls to show the effect of environment polarity and viscosity on TL mobility and $2a_N$ value.

Fig. 6 shows the EPR spectra of the TL loaded implants in the dry state and after different exposure times to PBS. The EPR spectrum of the Tempol in PBS is shown to make the comparison easier.

As can be seen in Fig. 6, the EPR spectra of the TL loaded implants in the dry state do not show real powder like spectra like what was observed in the dry state of TB loaded implants. The three broad lines of these spectra show that most part of TL shows moderate mobility (indicating mobility in a viscous environment) even before exposure to buffer. Due to their different hydrophilicities, TL and TB will localize in different environments in heterogeneous media. TL is much more hydrophilic and we hypothesised that three line spectrum of TL arises from the localization in viscous microregions of high polarity (e.g. adsorbed water). This assumption has been confirmed by the evaluation of the hyperfine splitting values.

The distance between the first and the third line ($2a_N$) is sensitive to the polarity of the environment. The $2a_N$ values for both TL loaded implants in the dry state are 3.43 mT which is close to the $2a_N$ value of TL in PBS ($=3.46$ mT), but much higher than the $2a_N$ values for TL in olive oil ($2a_N = 3.15$ mT) and NMP ($2a_N = 3.21$ mT) (Fig. 7). After exposure of both TL loaded extrudates to PBS, a continuous decrease in the width of all three lines was observed over the whole time period, but the most remarkable change was already observed only after 5 min.

These results prove a very fast water penetration into both systems (Fig. 7). These results are in line with the results obtained from the EPR

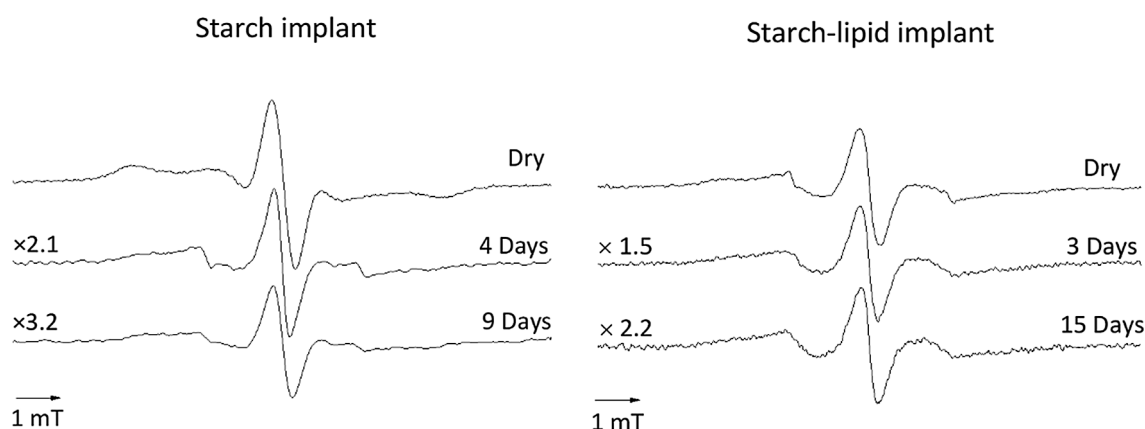


Fig. 4. EPR-Spectra of Tempol benzoate (TB) loaded implants. Starch implant on the left, and, starch-lipid implant on the right, after different times of exposure to PBS.

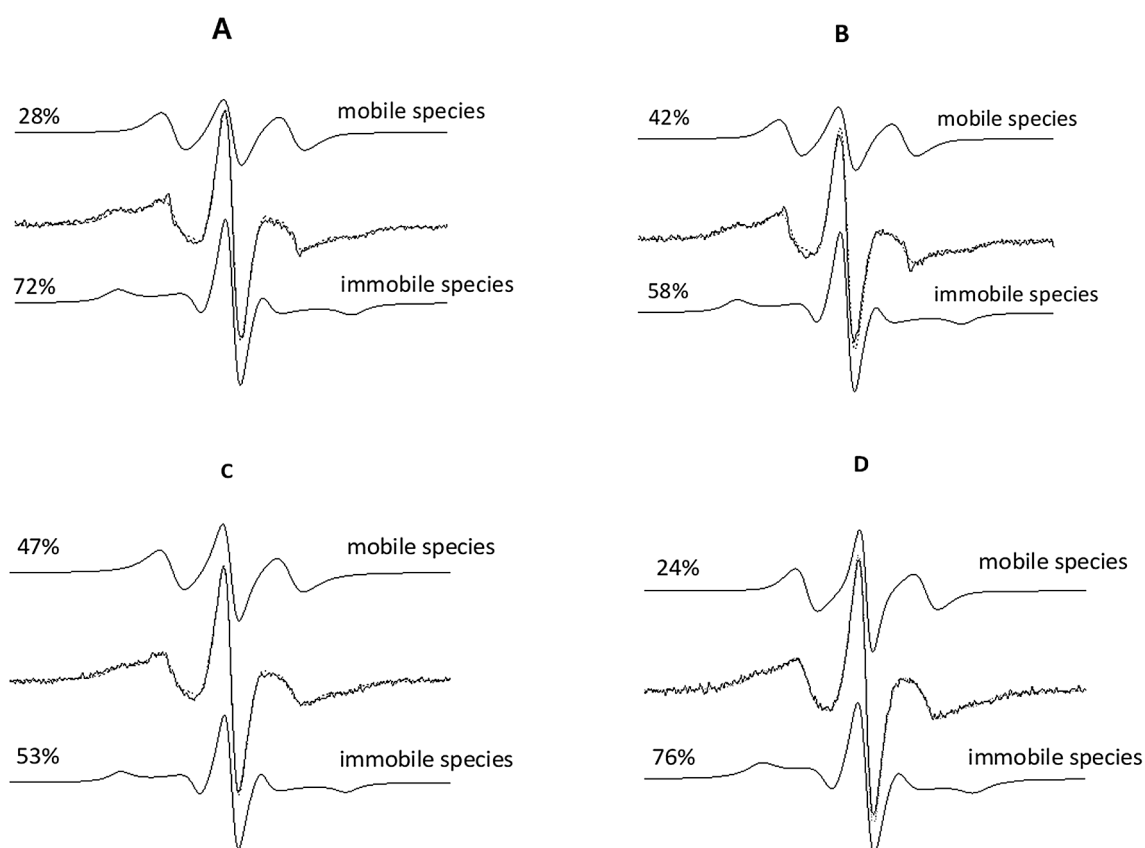


Fig. 5. EPR spectra of TB loaded starch-lipid implant exposed to PBS (black) after different exposure times to PBS and simulation (dashed line) of the mobile and immobile spectral pattern. The figure shows EPR spectra of the implant after: 5 min (a), 15 min (b), 24 h (c) and, 48 h (d) exposure to PBS.

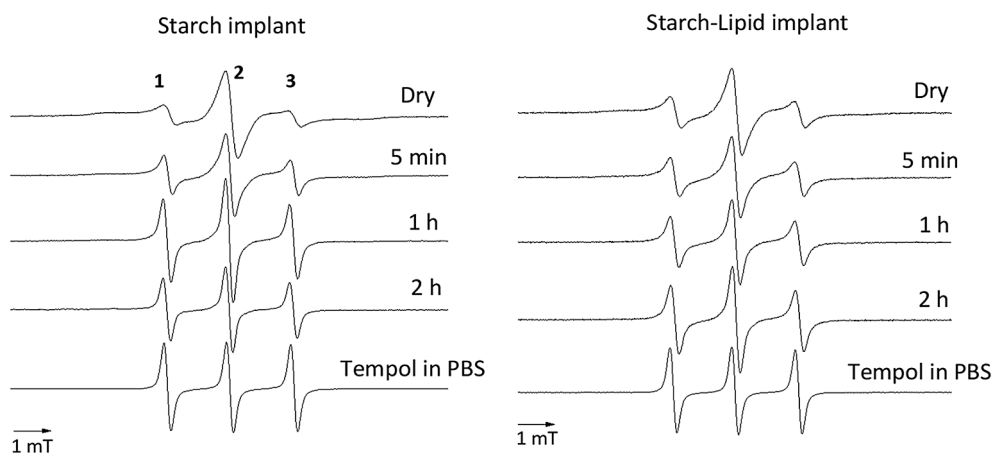


Fig. 6. EPR-Spectra of TL loaded implants (starch implant on the left and starch-lipid implant on the right) after different times of exposure to PBS.

spectra simulation. Both experiments demonstrated a fast water diffusion into the systems in the first 5 min and a subsequent increase in the amount of solubilized spin probe inside the implant that is released over time.

Based on the results of EPR experiments, both the starch implant and starch-lipid implant demonstrated the potential to be used as a controlled release system for more lipophilic drugs. Hydrophilic small molecules are expected to be released similar to TL. The EPR spectra of the TL extrudates prove a fast water penetration and solubilization of hydrophilic molecules both in GMS loaded extrudates and GMS free extrudates.

In order to assess the effect of the amount of lipid (GMS) on the

system's characteristics, three formulations including starch implant, starch-low lipid implant, and, starch-high lipid implant were produced and characterized. The exact components of each formulation are shown in Table 1.

3.4. Texture analysis

Subcutaneous injection is a possible route of administration for the prepared implants. For subcutaneous injection, it is important to have an implant with sufficient flexibility and mechanical resistance. A brittle implant may break during insertion, therefore, sufficient strength is required to withstand the insertion process. Breakage or cracks in the

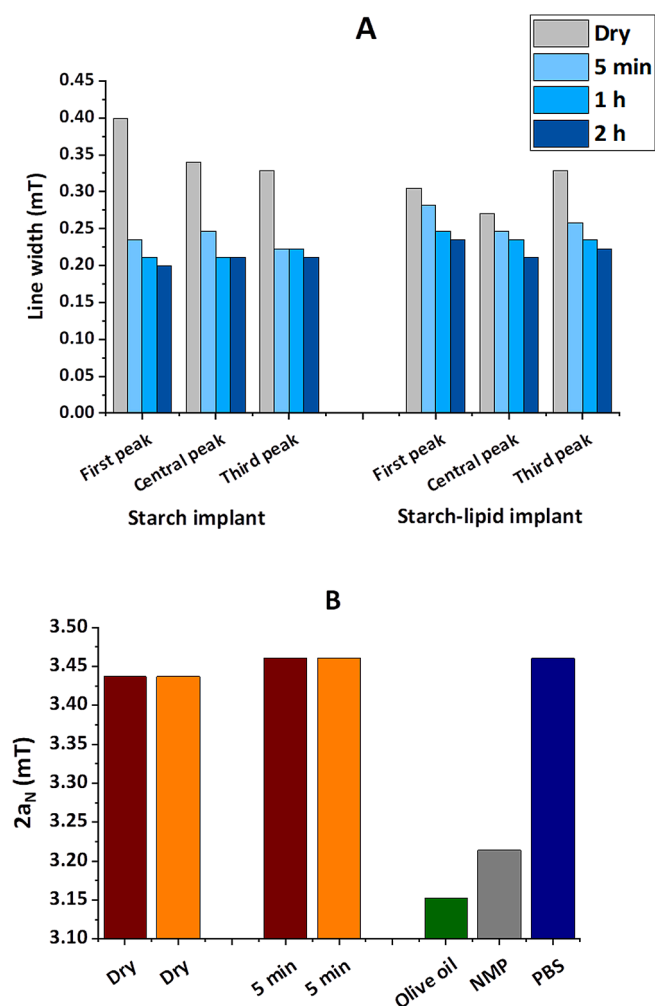


Fig. 7. A: Impact of buffer incubation time on EPR line widths. B: The $2a_N$ hyperfine splitting values for TL loaded starch implant and starch-lipid implant in the dry state ($2a_N = 3.43$ mT) and after 5 min exposure to PBS ($2a_N = 3.46$ mT). The $2a_N$ values for TL in olive oil ($2a_N = 3.15$ mT), NMP ($2a_N = 3.21$ mT) and PBS ($2a_N = 3.46$ mT). Typical standard deviations in the determination of the $2a_N$ values and the line widths were below 1% and 5% respectively.

implant may lead to faster release of drug and undesirable side effects in the patient. Different mechanical tests have been reported to assess the mechanical properties of medical devices. A test similar to the performed test in this study has been done by Lehner et al. to evaluate the

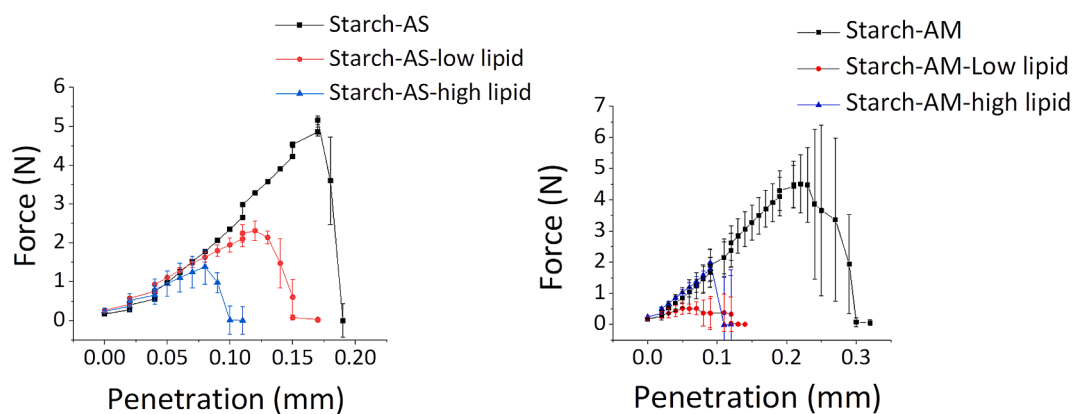


Fig. 8. Penetration test – Force path diagrams of implants loaded with artesunate (left) and artemether (right) with the same diameter of 1 mm; $n = 3$; the error bars indicate the standard deviation.

mechanical strength of intracochlear PLGA based implants for dexamethasone release (Lehner et al., 2019). In a study done by Stewart et al. a three-point bending test was performed to find the maximum force required to break the 3D printed biodegradable subcutaneous implants for prolonged drug delivery (Stewart et al., 2020). In this study, the mechanical properties of the implants were studied by texture analysis. A small blade was forced to penetrate over a distance of 0.3 mm into the implant and the resulting force was measured. Fig. 8 shows the force path diagrams of the different implants. All implants cracked before reaching the 0.3 mm penetration distance. Testing of starch implants resulted in a fast increase of force, indicating a higher mechanical resistance in comparison to lipid containing formulations. The maximum forces for the artesunate and artemether loaded starch implants were 5.15 N and 4.50 N respectively. The found maximum forces for lipid containing formulations were much lower than for the starch-based implants. They were for starch-low lipid and starch-high lipid implants 0.51 N and 1.98 N for artemether loaded implants, and 2.2 N and 1.38 N for artesunate loaded implants respectively. These formulations were all cracked before reaching a distance of 0.15 mm. As the results show, the addition of the lipid to the formulation makes the implants more brittle. The observed increase in the standard deviations at the final points of the graph is due to crack formation and breakage of the implants.

3.5. X-ray powder diffraction

Fig. 9 shows the x-ray pattern of the powdered samples. X-ray diffractograms of powdered samples of starch are shown in the supplementary (Fig. S6). Fig. 9 shows the diffractograms of artesunate, GMS and the formulations loaded with artesunate on the left and diffractograms of artemether, GMS and the formulations loaded with artemether on the right. Both antimalarial agents are crystalline powder. The diffractograms show the identical peaks of artesunate (Lisgarten et al., 2002) and artemether (Luo et al., 1984). The strong diffraction peaks of artesunate and artemether were observed in all formulations. Therefore, both drugs exist in their crystalline state in all formulations. The diffraction patterns of artesunate prove no polymorphic transformation to the second crystalline form. There are some changes in the diffraction patterns of artemether loaded starch implant and starch-low lipid implant. Further studies are needed to prove whether transformation to another crystalline form of artemether has occurred due to the heat, pressure and existence of water in the extrusion process (Gao et al., 2013; Zhang et al., 2011). Observed peaks with 2 Theta values of 8.9, 10.63 and 11.15° in GMS diffractogram correspond to d spacing values of 0.46, 0.38 and 0.37 nm that are the typical peaks of the beta crystalline form of the GMS, usually seen in the raw GMS powder (Himawan et al., 2006; Metin and Hartel, 2005). The x-ray diffractograms of the

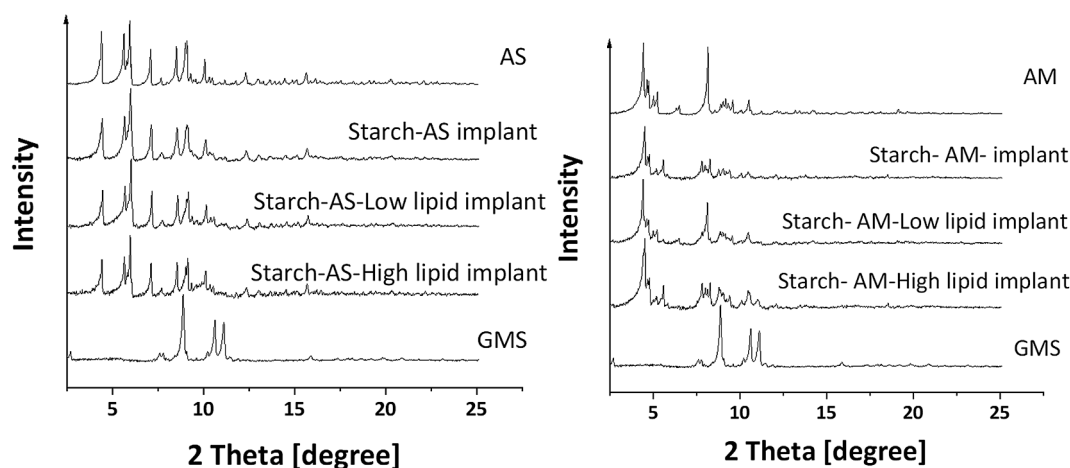


Fig. 9. XRPD-diffractograms of powdered samples of artesunate, artesunate loaded implants and GMS (left) and artemether, artemether loaded implants and GMS (right). The measurements were carried out at room temperature.

physical mixture of the GMS and other components of the formulation before the extrusion were also obtained which are shown in [supplementary materials](#) (Fig. S7 and Fig. S8). The GMS peaks were not clearly detectable in the physical mixture. Therefore, although the GMS peaks were not observed after the extrusion process, it cannot be concluded whether the GMS exist in its beta crystalline state after the extrusion process.

3.6. *In vitro* artesunate and artemether release

The release of artesunate and artemether from different formulations was investigated at 37 °C in PBS pH 7.4. Fig. 10 shows the artesunate and artemether release kinetics. As can be seen in the graphs, the release of the artesunate was completed after 2 days in all three formulations. No significant difference between the release behaviors can be seen. The addition of the lipid to the formulation did not cause significant changes in the release behaviour of artesunate. This is probably due to the effect of lipid (GMS), preventing the full starch gelatinization during the extrusion process. It might therefore also prevent possible interactions between the drug and the starch. Further studies are needed to understand the possible interactions between the components of the formulation. The total amount of released artesunate was equal to 3.0 mg ± 0.14 mg, 3.0 mg ± 0.20 mg and 3.1 mg ± 0.31 mg for the starch implant, starch-low lipid implant and starch-high lipid implant respectively. As can be seen in the graph, the released amount of the drug has not reached 100 percent of the loaded drug. This is probably due to the

hydrolysis of artesunate to dihydroartemisinin during the *in vitro* study. Several studies have shown that, in aqueous solutions, artesunate hydrolyzes to dihydroartemisinin (DHA), depending on the environmental conditions, including temperature and pH (Agnihotri et al., 2013; Batty et al., 1996; Gabriëls and Plaizier-Vercammen, 2004). Simultaneous quantification of artesunate and dihydroartemisinin in plasma by HPLC has been done by several studies (Chutvirasakul et al., 2021; Geditz et al., 2014). DHA co-exists in two forms and is shown as DHA-1 and DHA-2 in the chromatogram in supplementary (Fig. S9). Related peaks to DHA were observed in chromatograms of release media of all artesunate loaded implants (Fig. S9). Regarding the formulations loaded with artemether, the starch-high lipid implant was unstable in PBS plus 1% SDS and it was completely destroyed after a few hours. Therefore, the release behavior of this formulation was not assessed. Per WHO guidelines, treatment of severe malaria with artemether starts with a relatively high initial dose and continues with a maintenance dose for another 2 days. Both formulations of artemether showed a relatively high initial release continued with the constant release of the drug over several days. The drug was released from the starch-low lipid implant in 3 days, while the release was prolonged to 6 days from the starch implant. The total amount of released artemether from the implants were equal to 4.0 mg ± 0.08 mg and 4.0 mg ± 0.02 mg respectively which is of relevance to the therapeutics dose in preclinical studies in mice (Lin et al., 1994; Zech et al., 2021). The release profiles of both formulations match with a desired kinetic profile for the treatment of severe malaria per WHO guidelines (World Health Organization, 2015).

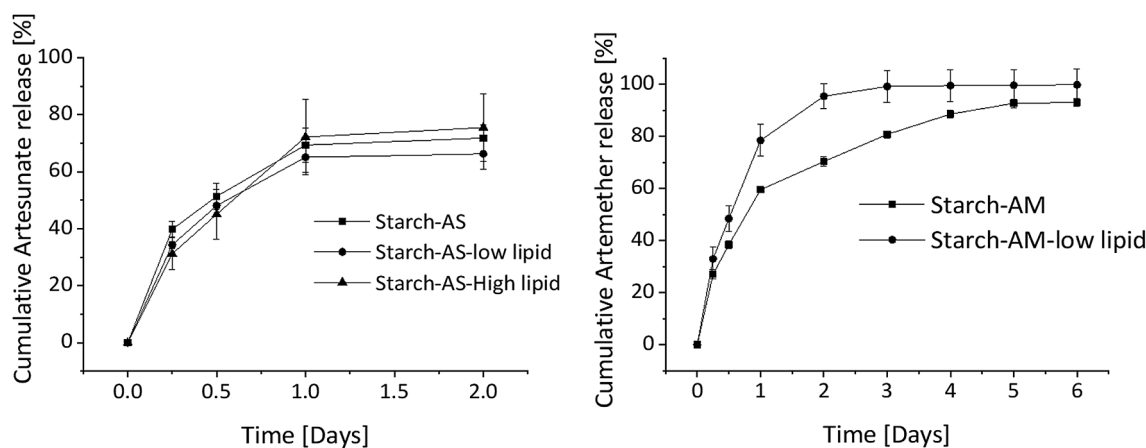


Fig. 10. Cumulative release of artesunate (left) and artemether (right) from different implants in PBS plus 1% SDS pH 7.4; n = 3; the error bars indicate the standard deviation.

Both Artemether and artesunate metabolize to the same active metabolite dihydroartemisinin in the human body. Also, per WHO guidelines artemether is the drug of choice for the treatment of severe malaria, in case parenteral artesunate is not available. Therefore, both artemether loaded implants (starch-AM implant and starch-AM-low lipid implant) are potential candidates for the treatment of severe malaria.

Based on the obtained data for the release kinetics, the addition of lipid to the formulations could not provide longer drug release from the implants. This is probably due to the high amount of drug loading (50%) that reduced the interactions between the lipid and starch and could also lead to porogenic effects. Further studies are needed to assess the possible interactions between the drug, starch and lipid in more detail. The EPR results and the drug release studies confirmed that the degree of benefit of combining starch and GMS will depend on (i) the selected ratio starch/GMS, the (ii) the drug properties and (iii) the drug load. The best benefit will be for drugs which are molecular dispersed in the lipid phase. This scenario is expected for lipophilic molecules at low loadings (e.g. as observed for TB in our study). Solid lipids are, due to their partially crystalline structure, only able to accommodate a limited amount of foreign molecules, even if they are hydrophobic. High drug loadings with hydrophobic drugs will therefore lead to phase separation and the formation of at least three different domains: (i) phase separated drug molecules, (ii) GMS phase with drug molecules dissolved and (iii) starch phase with an expected low amount of hydrophobic drug molecules.

4. Conclusion

This study investigates the possibility to combine different types of starch with GMS to produce a parenteral depot system, that can provide a sustained release of antimalarial agents over a few days to a week. In prescreening studies, the extrudability of the different starch varieties, formulated with different GMS proportions, were studied, in order to choose an appropriate starch, that can form a controlled release system complying with predefined characteristics. These characteristics include the implant's homogeneity, the physical stability in PBS and the release profile of the drug model (spin probes) from the prepared implant. Also, the temperature, the extrusion screw speed and the optimal water amount for the HME were optimized in prescreening studies. These studies showed the general feasibility to make a controlled release system as an implant, using high amylose starch and GMS. EPR studies confirmed the potential of the prepared system to provide a sustained release of the drug model over a period of a few days to weeks depending on the physicochemical properties of the loaded drug model. Therefore, three formulations including starch, starch-low lipid and starch-high lipid, loaded with antimalarial agents, artesunate and artemether, were produced and characterized. The results of the texture analysis demonstrated that, for both artesunate and artemether loaded formulations, starch implants had the maximum mechanical resistance and the addition of the lipid to the formulations makes the implant more brittle. The XRPD confirmed the crystalline state of both artesunate and artemether in all prepared implants. Artemether was released over a longer period of time in comparison to the artesunate. The release was completed after 3 days in starch-low lipid implant while it was prolonged to 6 days in starch implant. The release kinetics of both implants match the desired release profile for the treatment of severe malaria. Artemether and artesunate both metabolize to the same active metabolite dihydroartemisinin in the human body. Also, per WHO guidelines artemether is the drug of choice for the treatment of severe malaria, in case parenteral artesunate is not available (World Health Organization, 2015). Therefore, both formulations are potential candidates to be used in the treatment of severe malaria.

In summary, the study shows the general suitability of biodegradable starch-based implants in forming a sustained release system with desired mechanical properties.

CRediT authorship contribution statement

Golbarg Esfahani: Conceptualization, Methodology, Validation, Investigation, Writing – original draft. **Olaf Häusler:** Conceptualization, Writing – review & editing. **Karsten Mäder:** Conceptualization, Writing – review & editing, Resources, Supervision, Funding acquisition.

Declaration of Competing Interest

The authors declare that they have no known competing financial interests or personal relationships that could have appeared to influence the work reported in this paper: [Golbarg Esfahani reports financial support was provided by the European Union and the Federal State of Saxony-Anhalt. Karsten Mäder reports material supply (starch) was provided by Roquette Freres. Olaf Häusler reports a relationship with Roquette Freres that includes: employment.].

Acknowledgements

This study was supported by the IGS "Functional polymers" as a part of the AGRIPOLY program with funding from the European Social Fund (ESF). Additionally, we kindly thank Dr Christoph Wagner from the Chemistry Institute of Martin Luther University Halle-Wittenberg for his supports in x-ray diffraction measurements. As well, we would like to express our gratitude to the companies Roquette (Lestrem, France), BASF (Germany) and IOI Oleo GmbH (Germany) for providing us with the materials.

Appendix A. Supplementary material

Supplementary data to this article can be found online at <https://doi.org/10.1016/j.ijpharm.2022.121879>.

References

- Agnihotri, J., Singh, S., Bigonia, P., 2013. Formal chemical stability analysis and solubility analysis of artesunate and hydroxychloroquine for development of parenteral dosage form. *J. Pharm. Res.* 6 (1), 117–122.
- Klayman, D.L., Lin, A.J., Ager, A.L., 1994. Antimalarial activity of dihydroartemisinin derivatives by transdermal application. *Am. J. Trop. Med. Hyg.* 50 (6), 777–783.
- Alberta Araújo, M.A., Cunha, A.M., Mota, M., 2004. Enzymatic degradation of starch-based thermoplastic compounds used in protheses: identification of the degradation products in solution. *Biomaterials* 25 (13), 2687–2693.
- Batty, K.T., Ilett, K.F., Davis, M.E., 1996. Chemical stability of artesunate injection and proposal for its administration by intravenous infusion. *J. Pharm. Pharmacol.* 48 <https://doi.org/10.1111/j.2042-7158.1996.tb05870.x>.
- Besheer, A., Wood, K.M., Peppas, N.A., Mäder, K., 2006. Loading and mobility of spin-labeled insulin in physiologically responsive complexation hydrogels intended for oral administration. *J. Control. Release* 111 (1–2), 73–80.
- Bialleck, S., Rein, H., 2011. Preparation of starch-based pellets by hot-melt extrusion. *Eur. J. Pharm. Biopharm.* 79 (2), 440–448.
- Builders, P.F., Anwunobi, P.A., Mbah, C.C., Adikwu, M.U., 2013. New direct compression excipient from tigernut starch: physicochemical and functional properties. *AAPS PharmSciTech* 14 (2), 818–827.
- Castro, L.M.G., Alexandre, E.M.C., Saraiva, J.A., Pintado, M., 2020. Impact of high pressure on starch properties: a review. *Food Hydrocoll* 106, 105877.
- Chutvirasakul, B., Joseph, J.F., Parr, M.K., Suntornasuk, L., 2021. Development and applications of liquid chromatography-mass spectrometry for simultaneous analysis of anti-malarial drugs in pharmaceutical formulations. *J. Pharm. Biomed. Anal.* 195, 113855.
- Cui, R., Oates, C.G., 1999. The effect of amylose-lipid complex formation on enzyme susceptibility of sago starch. *Food Chem.* 65 (4), 417–425.
- De Pilli, T., Giuliani, R., Buléon, A., Pontoire, B., Legrand, J., 2016. Effects of protein-lipid and starch-lipid complexes on textural characteristics of extrudates based on wheat flour with the addition of oleic acid. *Int. J. Food Sci. Technol.* 51 (5), 1063–1074.
- Ding, A.G., Schwendeman, S.P., 2008. Acidic microclimate pH Distribution in PLGA microspheres monitored by confocal laser scanning microscopy. *Pharm. Res.* 25 (9), 2041–2052.
- Donmez, D., Pinho, L., Patel, B., Desam, P., Campanella, O.H., 2021. Characterization of starch-water interactions and their effects on two key functional properties: starch gelatinization and retrogradation. *Curr. Opin. Food Sci.* 39, 103–109.
- Esu, E.B., Effa, E.E., Opie, O.N., Meremikwu, M.M., Berbenetz, N., 2020. Artemether for severe malaria. *Emergencias*. <https://doi.org/10.1002/14651858.CD010678.pub3>.

- Evans, R.G., Wain, A.J., Hardacre, C., Compton, R.G., 2005. An electrochemical and ESR spectroscopic study on the molecular dynamics of TEMPO in room temperature ionic liquid solvents. *ChemPhysChem* 6 (6), 1035–1039.
- Gabriëls, M., Plaizier-Vercammen, J., 2004. Experimental designed optimisation and stability evaluation of dry suspensions with artemisinin derivatives for paediatric use. *Int. J. Pharm.* 283 (1–2), 19–34.
- Gao, H., Chen, L., Chen, W., Bao, S., 2013. Thermal stability evaluation of β -artemether by DSC and ARC. *Thermochim. Acta* 569, 134–138.
- Geditz, M.C.K., Heinkele, G., Ahmed, A., Kremsner, P.G., Kerb, R., Schwab, M., Hofmann, U., 2014. LC-MS/MS method for the simultaneous quantification of artesunate and its metabolites dihydroartemisinin and dihydroartemisinin glucuronide in human plasma. *Anal. Bioanal. Chem.* 406 (17), 4299–4308.
- Gelders, G.G., Duyck, J.P., Goesaert, H., Delcour, J.A., 2005. Enzyme and acid resistance of amylose-lipid complexes differing in amylose chain length, lipid and complexation temperature. *Carbohydr. Polym.* 60 (3), 379–389.
- Himawan, C., Starov, V.M., Stapley, A.G.F., 2006. Thermodynamic and kinetic aspects of fat crystallization. *Adv. Colloid Interface Sci.* 122 (1–3) <https://doi.org/10.1016/j.cis.2006.06.016>.
- Kempe, S., Mäder, K., 2012. In situ forming implants - An attractive formulation principle for parenteral depot formulations. *J. Control. Release.* 161 (2), 668–679.
- Kempe, S., Metz, H., Mäder, K., 2010. Application of Electron Paramagnetic Resonance (EPR) spectroscopy and imaging in drug delivery research - Chances and challenges. *Eur. J. Pharm. Biopharm.* 74 (1), 55–66.
- Klug, C.S., Feix, J.B., 2008. Methods and applications of site-directed spin labeling EPR spectroscopy. *Methods Cell Biol.* [https://doi.org/10.1016/S0091-679X\(07\)84020-9](https://doi.org/10.1016/S0091-679X(07)84020-9).
- Krämer, B., Neis, F., Brucker, S.Y., Kommos, S., Andress, J., Hoffmann, S., 2021. Peritoneal Adhesions and their Prevention. *Curr. Trends Surg. Technol. Int.* <https://doi.org/10.52198/21.sti.38.hr1385>.
- Kuntworbe, N., Acquah, F.A., Johnson, R., Ofori-Kwakye, K., 2018. Comparison of the physicochemical properties and in vivo bioavailability of generic and innovator artemether-lumefantrine tablets in Kumasi, Ghana. *J. Pharm. Pharmacogn. Res.* 6.
- Lehner, E., Gündel, D., Liebau, A., Plontke, S., Mäder, K., 2019. Intracochlear PLGA based implants for dexamethasone release: challenges and solutions. *Int. J. Pharm.: X* 1, 100015.
- Lisgarten, J.N., Potter, B., Palmer, R.A., Chimanuka, B., Aymami, J., 2002. Structure, absolute configuration, and conformation of the antimalarial drug artesunate. *J. Chem. Crystallogr.* 32 <https://doi.org/10.1023/A:1015696306812>.
- Lucke, A., Kiermaier, J., Göpferich, A., 2002. Peptide acylation by poly(α -hydroxy esters). *Pharm. Res.* 19 <https://doi.org/10.1023/A:1014272816454>.
- Luo, X.-D., Yeh, H.J.C., Bossi, A., Flippen-Anderson, J.L., Gillardi, R., 1984. The chemistry of drugs part IV, Configurations of antimalarials derived from qinghaosu: dihydroqinghaosu, artemether, and artesunic acid. *Helv. Chim. Acta* 67 (6), 1515–1522.
- Lurie, D., Mader, K., 2005. Monitoring drug delivery processes by EPR and related techniques - Principles and applications. *Adv. Drug Deliv. Rev.* 57 (8), 1171–1190.
- Mäder, K., Gallez, B., Liu, K.J., Swartz, H.M., 1996. Non-invasive in vivo characterization of release processes in biodegradable polymers by low-frequency electron paramagnetic resonance spectroscopy. *Biomaterials* 17 (4), 457–461.
- Mendes, S.C., Reis, R.L., Bovell, Y.P., Cunha, A.M., van Blitterswijk, C.A., de Bruijn, J.D., 2001. Biocompatibility testing of novel starch-based materials with potential application in orthopaedic surgery: a preliminary study. *Biomaterials* 22 (14), 2057–2064.
- Metin, S., Hartel, R.W., 2005. Crystallization of Fats and Oils. *Bailey's Industrial Oil and Fat Products*. doi:10.1002/047167849x.bio021.
- Morris, C.A., Duparc, S., Borghini-Fuhrer, I., Jung, D., Shin, C.-S., Fleckenstein, L., 2011. Review of the clinical pharmacokinetics of artesunate and its active metabolite dihydroartemisinin following intravenous, intramuscular, oral or rectal administration. *Malar. J.* 10 (1) <https://doi.org/10.1186/1475-2875-10-263>.
- Sasaki, T., Yasui, T., Matsuki, J., 2000. Effect of amylose content on gelatinization, retrogradation, and pasting properties of starches from waxy and nonwaxy wheat and their F1 seeds. *Cereal Chem.* 77 (1), 58–63.
- Schädlich, A., Kempe, S., Mäder, K., 2014. Non-invasive in vivo characterization of microclimate pH inside in situ forming PLGA implants using multispectral fluorescence imaging. *J. Control. Release* 179, 52–62.
- Stewart, S., Domínguez-Robles, J., McClorum, V., Mancuso, E., Lamprou, D., Donnelly, R., Larrañeta, E., 2020. Development of a biodegradable subcutaneous implant for prolonged drug delivery using 3D printing. *Pharmaceutics* 12 (2), 105.
- World Health Organization, 2020. World Malaria Report: 20 years of global progress and challenges, World Health.
- World Health Organization, 2015. Guidelines for the treatment of malaria Third edition. *Trans. R. Soc. Trop. Med. Hyg.* 85. [https://doi.org/10.1016/0035-9203\(91\)90261-V](https://doi.org/10.1016/0035-9203(91)90261-V).
- Zech, J., Dzikowski, R., Simantov, K., Golenser, J., Mäder, K., 2021. Transdermal delivery of artemisinins for treatment of pre-clinical cerebral malaria. *Int. J. Parasitol. Drugs Drug Resist.* 16, 148–154.
- Zhang, Y., Liu, Q., Zhang, D., Jiang, Y., 2011. Polymorphism, crystal structure and crystal habit of β -artemether. *Huagong Xuebao/CIESC J.* 62 <https://doi.org/10.3969/j.issn.0438-1157.2011.10.040>.